

Electronic Supplementary Information

Structure and Reactivity of Triflimide-Bridged Bis(Trimethylsilyl) Cation

*Joshua H. Daum, Nattamai Bhuvanesh, and Oleg V. Ozerov**

Department of Chemistry, Texas A&M University, 3255 TAMU, College Station, TX 77842.

*Email: ozero@chem.tamu.edu; Phone: +1-979-845-5870

Table of Contents

I. General Considerations	3
II. Synthesis of Compounds	4
III. Solubility Test	7
IV. Equilibrium Experiment	16
V. Characterization Details	25
VI. X-Ray Structural Analysis	32
VII. References	34

I. General Considerations

Unless otherwise specified all manipulations were performed under an atmosphere of Ar using a standard Schlenk line, a Lewis base-free glovebox (does not contain volatile Lewis base-containing compounds and is free of donor solvents). Toluene (PhMe), pentane, isooctane were dried and deoxygenated (by sparging with Ar) using an Innovative Technologies MD-5 solvent purification system and stored over molecular sieves in an Ar-filled glovebox. Benzene, d_6 -benzene (C_6D_6), d_8 -toluene (C_7D_8), fluorobenzene (PhF), Me_3SiOTf , allyltrimethylsilane, and tetramethylsilane (TMS) were dried over CaH_2 then vacuum transferred and then stored over molecular sieves in an Ar-filled glovebox. Orthodichlorobenzene (ODCB) and cyclohexane (C_6H_{12}) were dried over CaH_2 and then distilled, sparged with argon, and then stored over molecular sieves in an Ar-filled glovebox. SO_2Cl_2 was fractionally distilled, deoxygenated (via freeze pump thawing), and stored in an Ar-filled glovebox. $[(Me_3Si)_2OTf][HCB_{11}Cl_{11}]$ and $F_{15}Tr-OTFA$ was synthesized according to previous literature procedures.^{1,2} All other chemicals were used as received from commercial vendors.

All NMR spectra were recorded on a Bruker Avance 400 spectrometer (1H NMR, 400.200 MHz; ^{13}C NMR, 100.630 MHz; ^{11}B NMR, 128.400 MHz, ^{29}Si NMR, 79.490 MHz) and Bruker Avance 500 spectrometer (1H NMR, 500.13 MHz; ^{13}C NMR, 125.77 MHz; ^{11}B NMR, 160.462 MHz). Chemical shifts are reported in δ (ppm). For 1H and ^{13}C NMR spectra, the residual solvent peak was used as an internal reference or by externally referencing $\delta = 0$ ppm using $SiMe_4$. $^{11}B\{^1H\}$ NMR spectra were referenced externally to $\delta = 0$ ppm by using $BF_3 \cdot Et_2O$. ^{19}F NMR spectra were referenced externally to $\delta = -78.5$ ppm using neat CF_3COOH . ^{29}Si NMR spectra were referenced internally to $\delta = 0$ ppm using $SiMe_4$. IR spectra were taken on an Agilent Cary 630 FTIR spectrometer located in an argon-filled glovebox.

II. Synthesis of Compounds

[(Me₃Si)₂NTf₂][HCB₁₁Cl₁₁]. Method A. In a 25 mL Teflon capped flask, Tf₂NH (202 mg, 0.72 mmol) and allyltrimethylsilane (0.57 mL, 3.58 mmol) were stirred together for 2 hours before being placed under dynamic vacuum for 1 hour. Fluorobenzene (2 mL) and [Ph₃C][HCB₁₁Cl₁₁] (138 mg, 0.18 mmol) were then added to the flask before sealing the vessel and removing it from the glovebox. The flask was degassed over the course of 3 freeze-pump-thaw cycles and refilled with Me₃SiH (ca. 1 atm). Immediate color change was observed to a pale pink, and the solution was stirred overnight at ambient temperatures. The flask was transferred to a glovebox and the remaining solution was moved to a pre-weighed 20 mL scintillation tube with a stir bar. Pentane (10 mL) was subsequently added to the vessel and stirred rigorously whereupon a pale pink precipitate and clear, colorless supernatant was seen. The supernatant was decanted and the solid product was washed twice with 2 mL of pentane and allowed to dry *in vacuo* for about 1 minute until the solid looked dry (157 mg, 93% yield). **Method B.** To a 25 mL Teflon capped flask, Tf₂NH (40 mg, 0.14 mmol) and [Ph₃C][HCB₁₁Cl₁₁] (50 mg, 0.06 mmol) were combined with fluorobenzene (ca ~1 mL) and stirred. The flask was then sealed, removed from the glovebox, degassed over the course of 3 freeze-pump-thaw cycles, and refilled with Me₃SiH (ca. 1 atm). The solution immediately became colorless and the solution was stirred overnight. The flask was transferred to a glovebox and the remaining solution was moved to a pre-weighed 20 mL scintillation tube. Pentane (10 mL) was added and the vessel was stirred rigorously hereupon a white precipitate and clear, colorless supernatant was seen. The supernatant was decanted and the solid product was washed twice with 2 mL of pentane and allowed to dry *in vacuo* (60 mg, 99% yield). ¹H NMR (400 MHz, ODCB): δ 3.05 (s, 1H, carborane C-H), 0.53 (s, 18H, SiMe₃) ppm. ¹³C{¹H} NMR (101 MHz, ODCB): δ 123 (q, J_{C-F} = 322 Hz, CF₃), 0.43 (s, SiMe₃) ppm. ¹⁹F NMR

(162 MHz, ODCB): δ -75.8 (s) ppm. $^{11}\text{B}\{^1\text{H}\}$ NMR (128 MHz, ODCB): δ -3.1 (s, 1B), -10.7 (s, 5B), -13.9 (s, 5B) ppm. $^{29}\text{Si}\{^1\text{H}\}$ NMR (79 MHz, ODCB): δ 73.1 (s) ppm.

Reaction of [(Me₃Si)₂NTf₂][HCB₁₁Cl₁₁] with F₁₅Tr-OTFA to form [F₁₅Tr][HCB₁₁Cl₁₁]. The title compound was synthesized analogously according to a modified procedure.² In a 25 mL Schlenk flask with a stir bar, F₁₅Tr-OTFA (135 mg, 0.215 mmol) was dissolved in 10 mL of SiCl₄. [(Me₃Si)₂NTf₂][HCB₁₁Cl₁₁] (203 mg, 0.214 mmol) was added to the mixture resulting in a rapid color change to pink. The mixture gradually changed colors from light pink to dark purple, which then precipitated out of solution. The solution was allowed to for 3 h before being collected on a fine frit. The solid was washed with SiCl₄ (5 × 10 mL) before being dried *in vacuo* (133 mg, 60% yield). Subsequent ¹⁹F NMR analysis showed >94% purity.

III. Solubility Test

General Procedure for Measuring the Solubility of [(Me₃Si)₂NTf₂][HCB₁₁Cl₁₁] and

[(Me₃Si)₂OTf][HCB₁₁Cl₁₁]: A stock solution consisting of cyclohexane and perfluorobenzene was prepared in a solvent system of choice by weighing both into a volumetric flask. In a J. Young tube, 500 μL of the chosen solvent was mixed with either [(Me₃Si)₂NTf₂][HCB₁₁Cl₁₁] or [(Me₃Si)₂OTf][HCB₁₁Cl₁₁] until the solution becomes saturated and there remained undissolved solids/oil. ¹H and ¹⁹F NMR spectra were then taken and the concentration was determined by comparing the silylium NMR integrations to the internal standard.

Table S1. Solubility experiment data for [(Me₃Si)₂NTf₂][Cl₁₁] and [(Me₃Si)₂NTf₂][Cl₁₁].

Solvent	Silylium Cation Identity	<i>c</i> -C ₆ H ₁₂ in Solution (mmol/mL)	C ₆ F ₆ in Solution (mmol/mL)	Solubility of Silylium (mmol/mL)	Solubility of Silylium (mg/mL)
C ₆ D ₆	[(Me ₃ Si) ₂ NTf ₂]	0.200	0.148	1.162	>1100
C ₆ D ₆	[(Me ₃ Si) ₂ OTf]	0.200	0.148	0.0002	0.16
pentane	[(Me ₃ Si) ₂ NTf ₂]	0.056	0.022	0.0014	1.3
pentane	[(Me ₃ Si) ₂ OTf]	0.056	0.022	<0.0001	<0.01

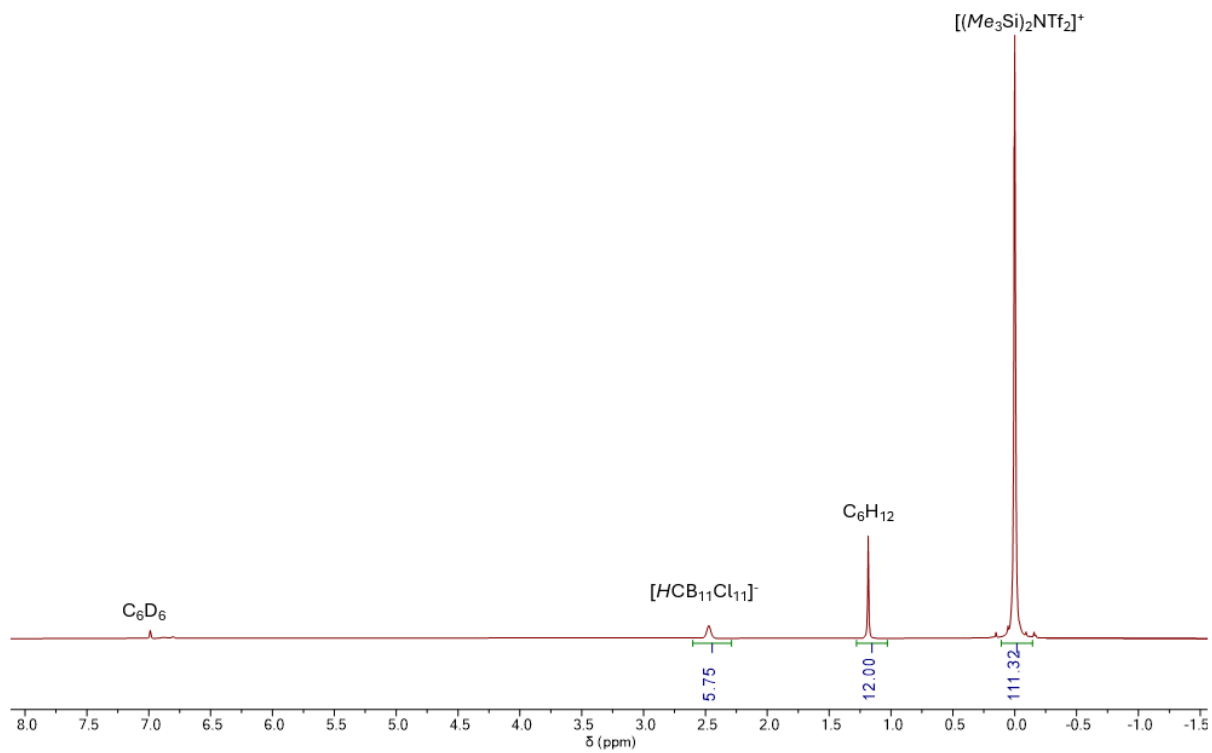


Figure S1. ^1H NMR (400 MHz, C_6D_6) spectrum of 551 mg of $[(\text{Me}_3\text{Si})_2\text{NTf}_2][\text{HCB}_{11}\text{Cl}_{11}]$ in 500 μL C_6D_6 .

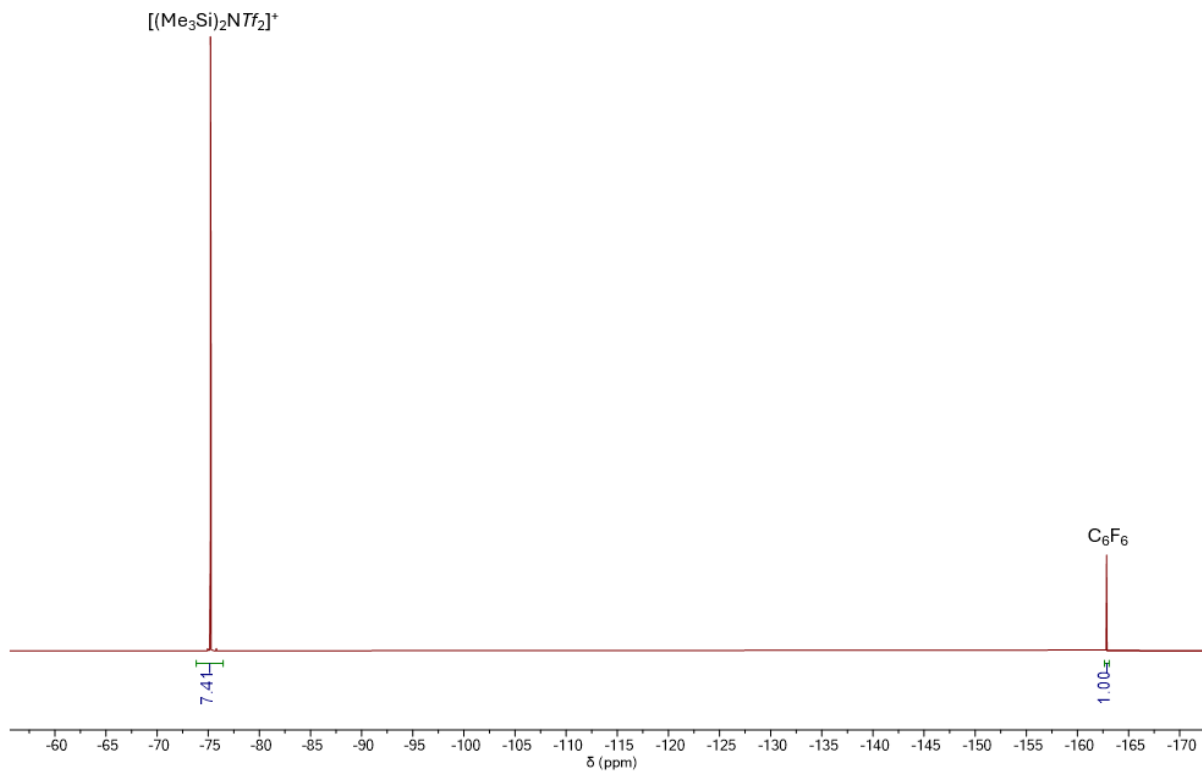


Figure S2. ^{19}F NMR (376 MHz, C_6D_6) spectrum of 551 mg of $[(\text{Me}_3\text{Si})_2\text{NTf}_2][\text{HCB}_{11}\text{Cl}_{11}]$ in 500 μL C_6D_6 .

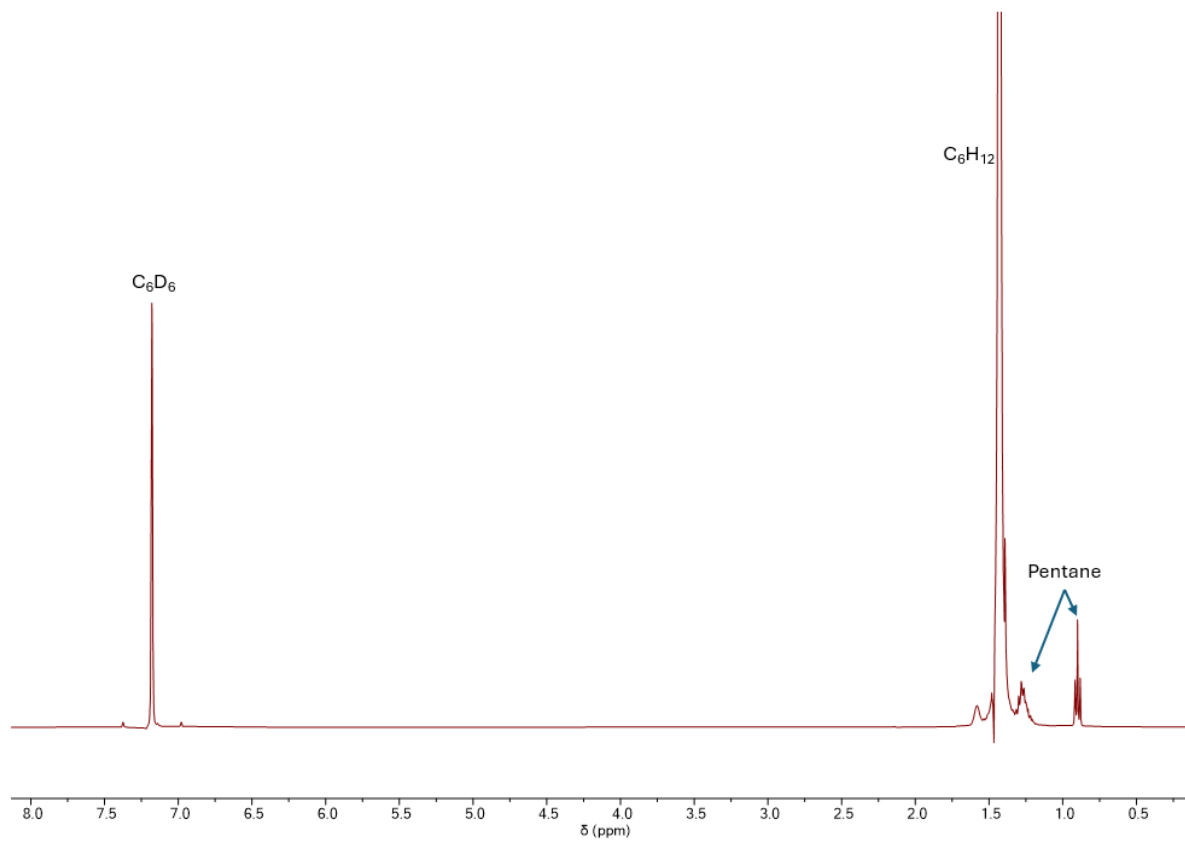


Figure S3. ^1H NMR (400 MHz, C_6D_6) spectrum of 0.08 mg of $[(\text{Me}_3\text{Si})_2\text{OTf}][\text{HCB}_{11}\text{Cl}_{11}]$ in 500 μL C_6D_6 . No silylium resonances were detected.

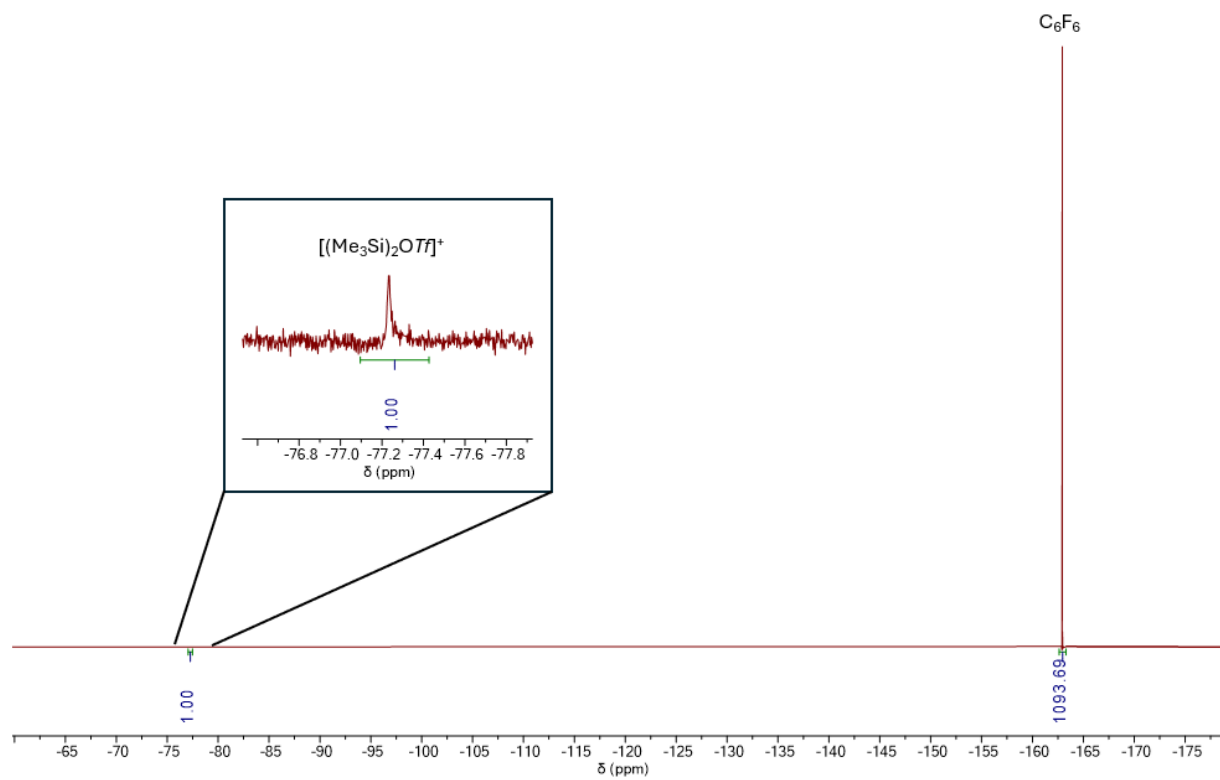


Figure S4. ^{19}F NMR (376 MHz, C_6D_6) spectrum of 0.08 mg of $[(\text{Me}_3\text{Si})_2\text{OTf}][\text{HCB}_{11}\text{Cl}_{11}]$ in $500 \mu\text{L}$ C_6D_6 .

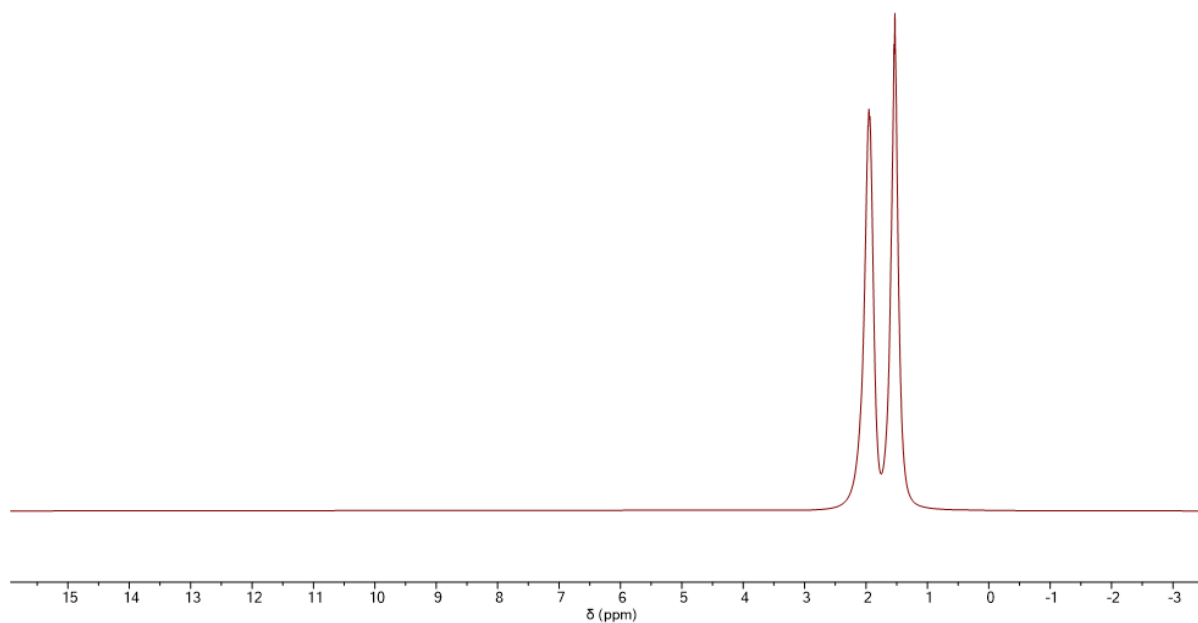


Figure S5. ¹H NMR (400 MHz, pentane, unlocked) spectrum of 0.72.7 mg of [(Me₃Si)₂NTf₂][HCB₁₁Cl₁₁] in 500 μL pentane. No characteristic silylium peaks could be detected.

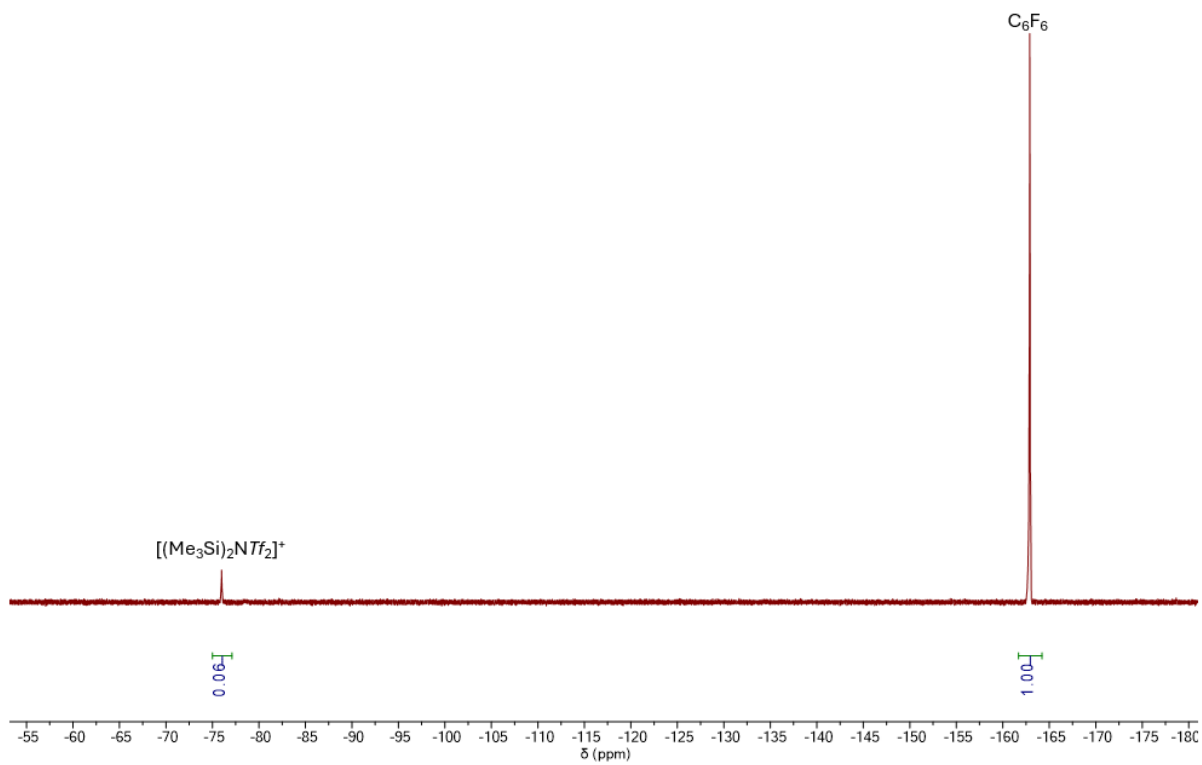


Figure S6. ^{19}F NMR (376 MHz, pentane, unlocked) spectrum of 0.7 mg of $[(\text{Me}_3\text{Si})_2\text{NTf}_2][\text{HCB}_{11}\text{Cl}_{11}]$ in 500 μL pentane.

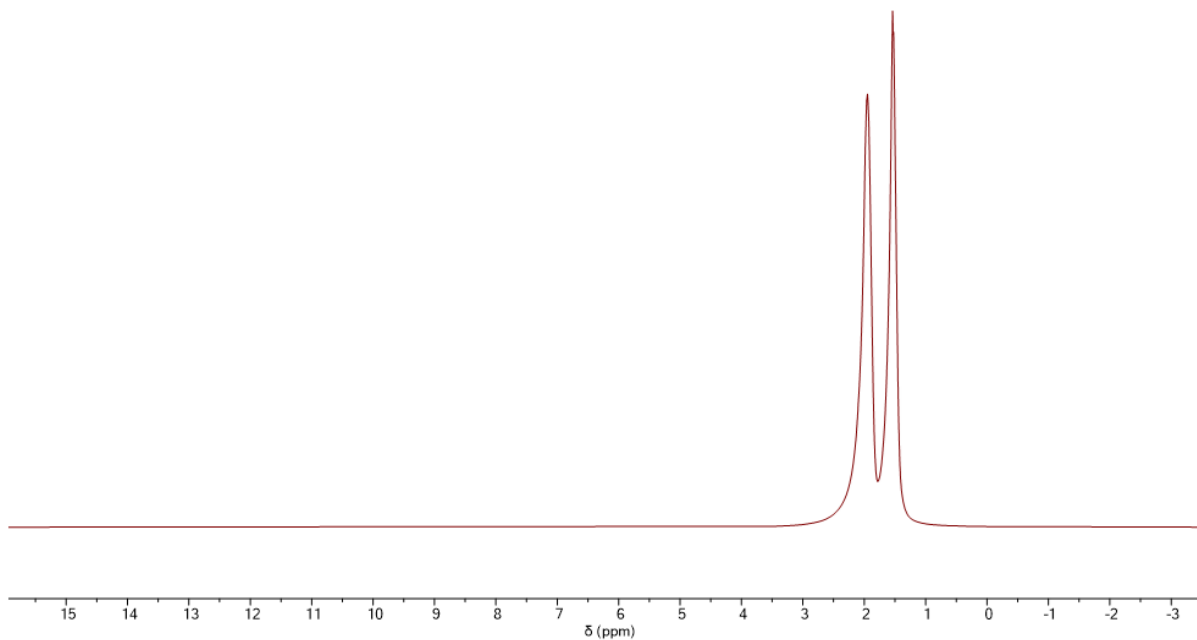


Figure S7. ^1H NMR (400 MHz, pentane, unlocked) spectrum of $[(\text{Me}_3\text{Si})_2\text{OTf}][\text{HCB}_{11}\text{Cl}_{11}]$ in 500 μL pentane. No characteristic silylium peaks could be detected.

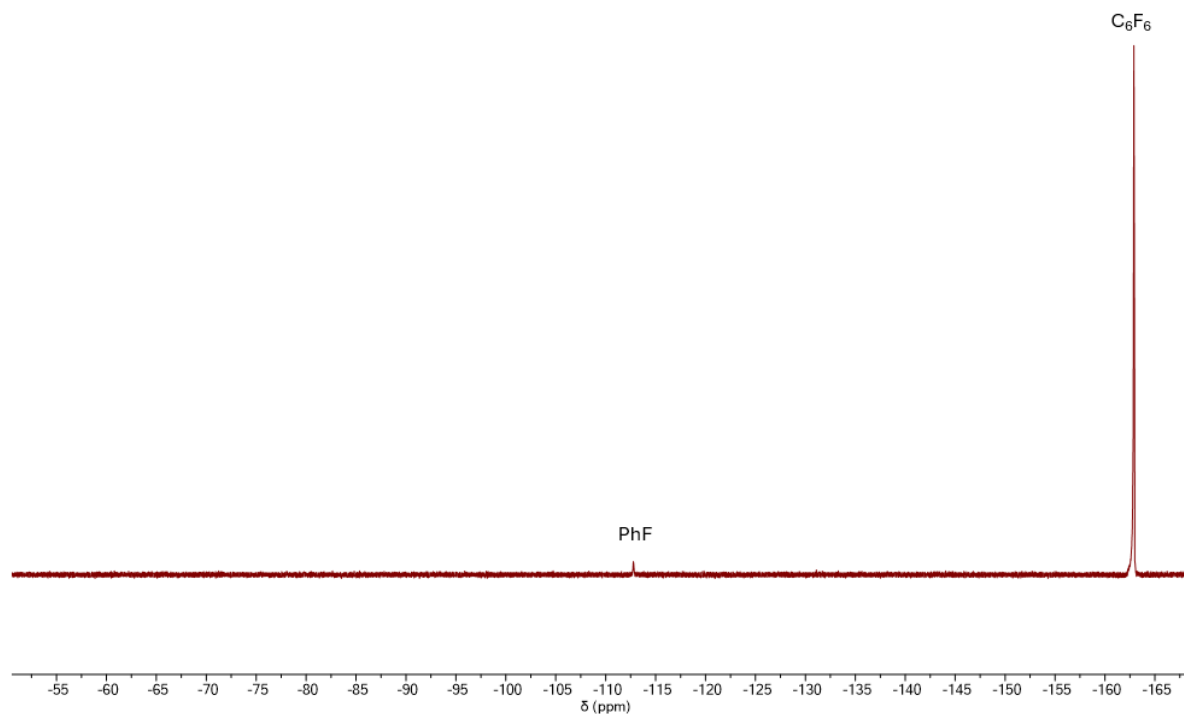


Figure S8. ^1H NMR (376 MHz, pentane, unlocked) spectrum of $[(\text{Me}_3\text{Si})_2\text{OTf}][\text{HCB}_{11}\text{Cl}_{11}]$ in 500 μL pentane. No characteristic silylium peaks could be detected. Trace PhF that is observed is carried over from the initial synthesis of $[(\text{Me}_3\text{Si})_2\text{OTf}][\text{HCB}_{11}\text{Cl}_{11}]$.

IV. Equilibrium Experiment

Mathematical approach. The mathematical approach assumes that the single peak observed in the $^{29}\text{Si}\{^1\text{H}\}$ NMR of the mixture of $[(\text{Me}_3\text{Si})_2\text{NTf}_2][\text{HCB}_{11}\text{Cl}_{11}]$ and Me_3SiOTf is due to a fast equilibrium shown below. We also assume that the exact chemical shift of the mixture is a weighted average of each of each component in the equilibrium $^{29}\text{Si}\{^1\text{H}\}$ chemical shifts. We also can determine the relative molar concentration of the species that contain NTf_2^- groups compared to the species that contain OTf^- by using their relative integration in ^{19}F NMR. As NTf_2^- has twice the number of fluorine atoms compared to OTf^- the measured integration value of NTf_2^- must be divided by 2 to obtain the relative molar concentration of the two species. This relative molar concentration also corresponds to the amount of $[(\text{Me}_3\text{Si})_2\text{NTf}_2][\text{HCB}_{11}\text{Cl}_{11}]$ and Me_3SiOTf initially used. We also know that the concentration of $[(\text{Me}_3\text{Si})_2\text{OTf}][\text{HCB}_{11}\text{Cl}_{11}]$ and $\text{Me}_3\text{SiNTf}_2$ must be the same as they must form in equal amounts. As such, a system of linear equations can be devised solving which can be solved to determine a K_{eq} .



Relative Concentration: $[A]$ $[B]$ $[C]$ $[D]$

$\delta^{29}\text{Si}\{^1\text{H}\}$ (ppm): a b c d

$x = \text{NTf}_2^-$ ^{19}F NMR relative integration in the mixture

$y = \text{OTf}^-$ ^{19}F NMR relative integration in the mixture

$z = \delta^{29}\text{Si}\{^1\text{H}\}$ (ppm) of the mixture

Equations:

$$[A]_{\text{initial}} = x/2 = [A] + [D]$$

$$z = \frac{a[A] + b[B] + c[C] + d[D]}{[A] + [B] + [C] + [D]}$$

$$[B]_{\text{initial}} = y = [B] + [C]$$

$$[C] = [D]$$

$$K_{\text{eq}} = \frac{[C][D]}{[A][B]}$$

Which could be rewritten algebraically to solve as:

$$= \frac{\frac{xz}{2} - \frac{xa}{2} + yz - yb}{c + d - a - b}$$

$$[B] = y - [C]$$

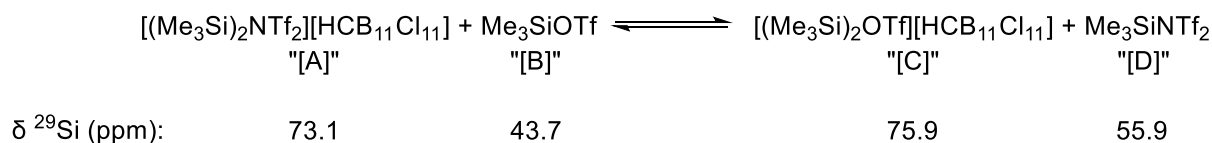
$$[A] = \frac{x}{2} - [C]$$

This system of equations was solved numerically in Microsoft Excel. For determining the ΔS and ΔH of the reaction, a Van't Hoff analysis was performed with the K_{eq} being calculated at every temperature (T) and the data being plotted as $\ln(K_{\text{eq}})$ vs. $1/T$. Using the LINEST function in Microsoft Excel, the slope of the line was used to determine ΔH and the y-intercept to determine ΔS . The Excel file with calculations is provided separately.

Error Assessment. The accuracy of the temperature measurements is estimated at ± 1 °C. Efforts were made to minimize systematic errors throughout the experimental procedure, e.g., using similar concentrations for all measurements. The $^{29}\text{Si}\{^1\text{H}\}$ NMR chemical shift of each species at various temperatures was independently determined with TMS always being referenced to 0 ppm. The standard error in the calculated K_{eq} values were determined via error propagation methods

using equations obtained from software developed by Gnyra³ (also see⁴ for the use of this program in scientific chemical literature) with the assumption that the standard error of measuring the ²⁹Si{¹H} chemical shift was 0.1 ppm and the integration values of NTf₂⁻ compared to OTf⁻ as determined by ¹⁹F NMR was ca. 5%. These initial error values were determined on the basis of subjective judgements on the precision of the instrument and by comparing the integration values of NTf₂⁻ to OTf⁻ over various temperatures. While calculating the ΔH and ΔS values using the LINEST function in Microsoft Excel, the estimated standard deviations were calculated. However, Excel does not consider the uncertainty in input experimental data such as those relating to temperature or K_{eq}. To account for the experimental uncertainty, the estimated standard deviations calculated by LINEST in MS Excel were increased by 400% and are reported as the error in the following tables. The Excel file with error calculations is provided separately.

Reaction of [(Me₃Si)₂NTf₂][HCB₁₁Cl₁₁] with Me₃SiOTf in ODCB. To a J. Young tube, [(Me₃Si)₂NTf₂][HCB₁₁Cl₁₁] (93.3 mg, 0.098 mmol) and SiMe₄ (10 μL) were dissolved in 800 μL of ODCB and fully characterized by NMR before the addition of Me₃SiOTf (~17.75 μL, 0.098 mmol). The mixture was analyzed by NMR again with the ¹⁹F NMR revealing the actual molar ratio of Me₃SiOTf that was added relative to [(Me₃Si)₂NTf₂][HCB₁₁Cl₁₁] was 0.95 to 1.0 respectively.



δ ²⁹Si Equilibrium Mixture: 64.9 ppm

Equations:

$$[A]_{\text{initial}} = 1 = [A] + [D]$$

$$[B]_{\text{initial}} = 0.95 = [B] + [C]$$

$$[C] = [D]$$

$$64.9 = \frac{73.1[A] + 43.7[B] + 75.9[C] + 55.9[D]}{[A] + [B] + [C] + [D]}$$

Solutions:

$$[A] = \frac{51}{250}, [B] = \frac{77}{500}, [C] = [D] = \frac{199}{250}$$

$$K_{eq} = \frac{[C][D]}{[A][B]} = 20 \pm 11$$

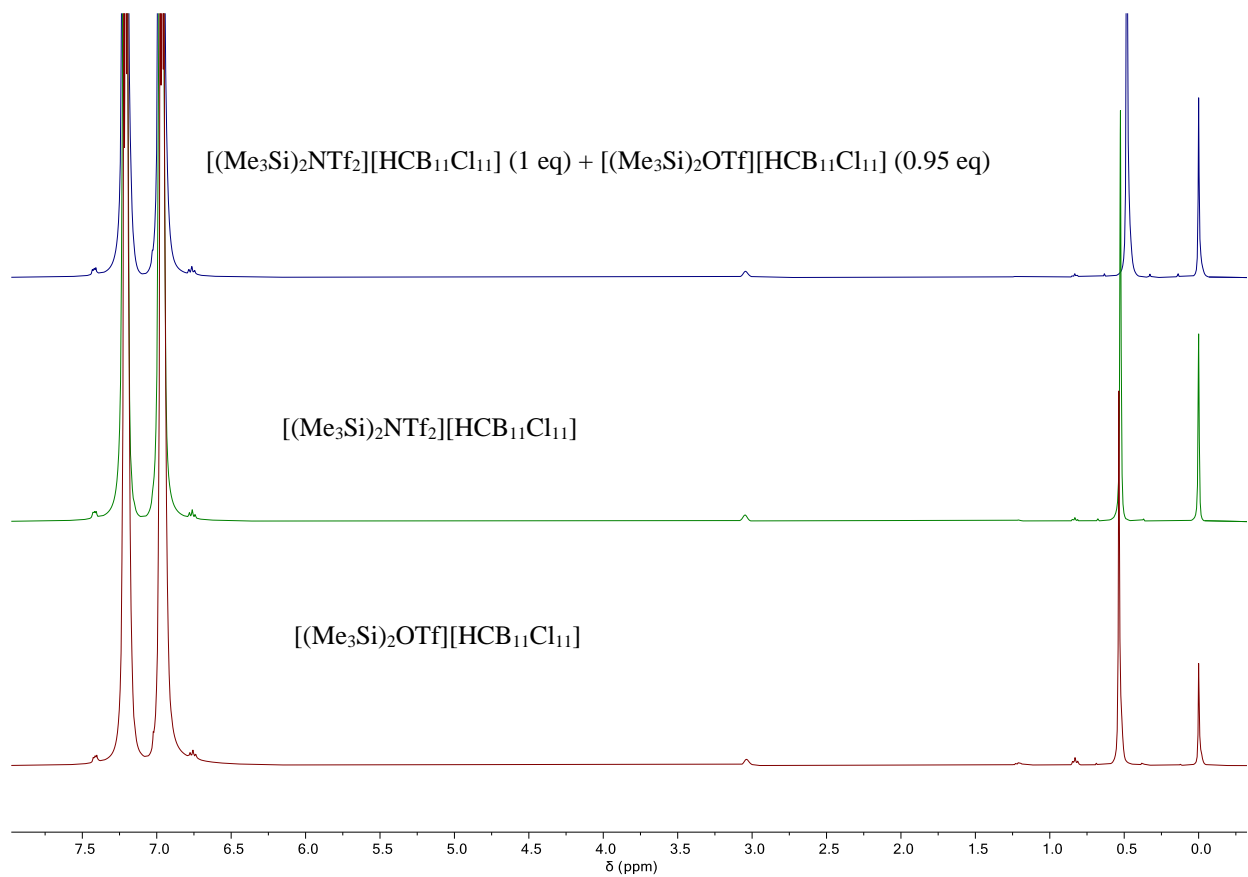


Figure S9. Stacked ¹H NMR (400 MHz/ODCB/unlocked) spectra of [(Me₃Si)₂OTf][HCB₁₁Cl₁₁], [(Me₃Si)₂NTf₂][HCB₁₁Cl₁₁], and a mixture of [(Me₃Si)₂NTf₂][HCB₁₁Cl₁₁] (1 eq) with Me₃SiOTf (0.95 eq). Note that SiMe₄ has been added as a reference.

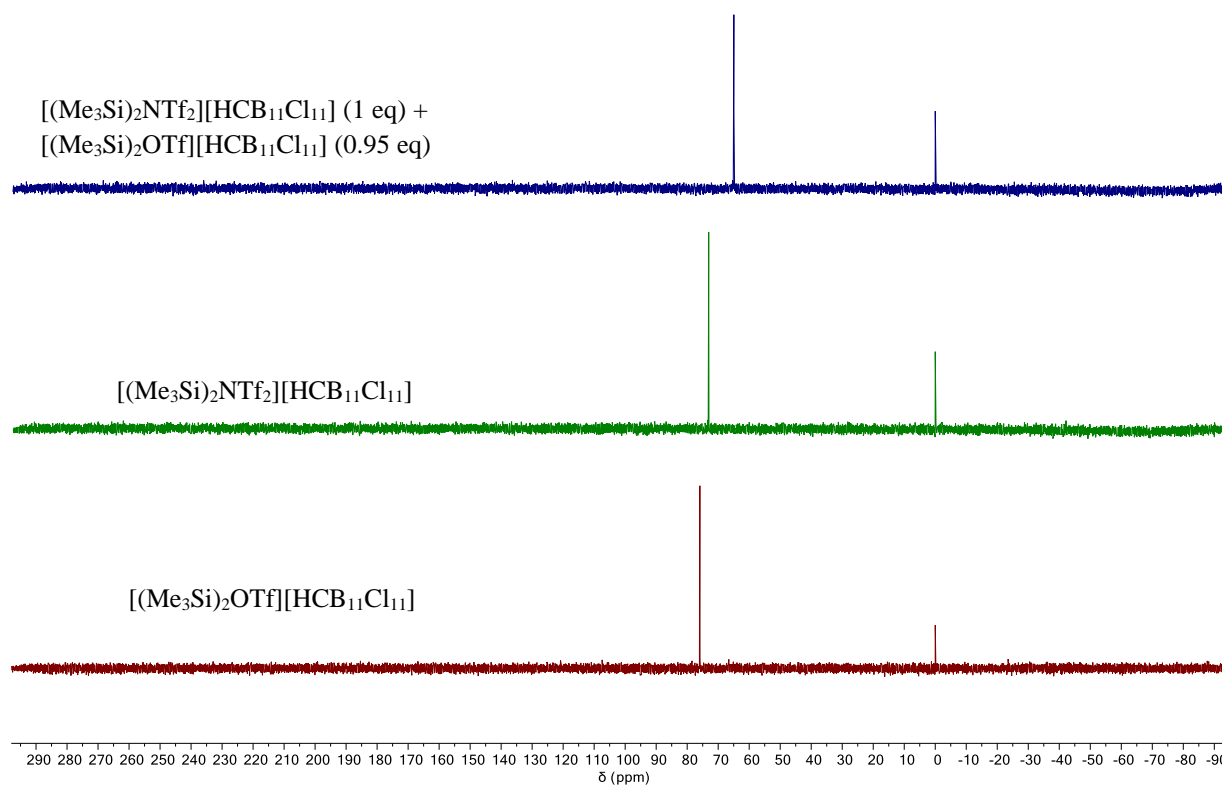


Figure S10. Stacked $^{29}\text{Si}\{^1\text{H}\}$ NMR (79 MHz/ODCB/unlocked) spectra of $[(\text{Me}_3\text{Si})_2\text{OTf}][\text{HCB}_{11}\text{Cl}_{11}]$, $[(\text{Me}_3\text{Si})_2\text{NTf}_2][\text{HCB}_{11}\text{Cl}_{11}]$, and a mixture of $[(\text{Me}_3\text{Si})_2\text{NTf}_2][\text{HCB}_{11}\text{Cl}_{11}]$ (1 eq) with Me_3SiOTf (0.95 eq). Note that SiMe_4 has been added as a reference.

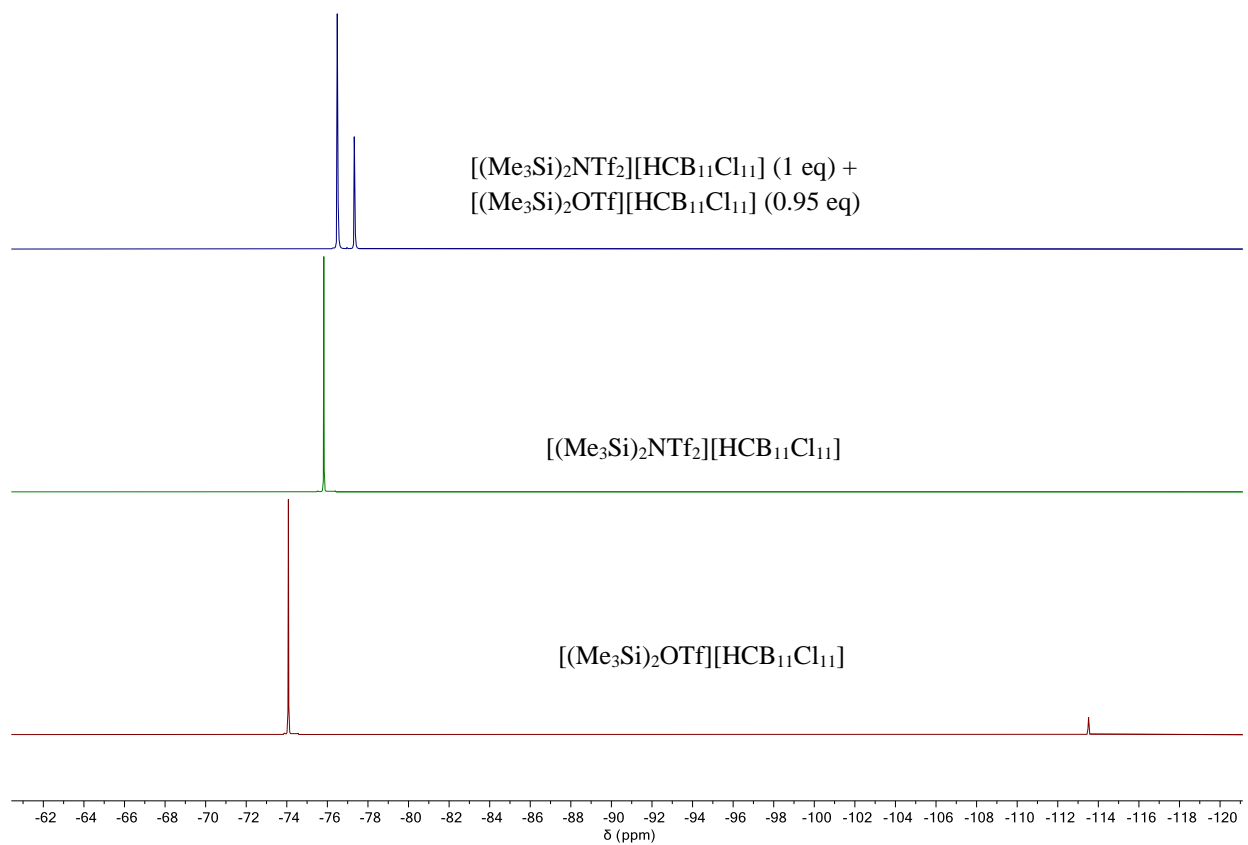


Figure S11. Stacked $^{19}\text{F}\{^1\text{H}\}$ NMR (471 MHz/ODCB/unlocked) spectra of $[(\text{Me}_3\text{Si})_2\text{OTf}][\text{HCB}_{11}\text{Cl}_{11}]$, $[(\text{Me}_3\text{Si})_2\text{NTf}_2][\text{HCB}_{11}\text{Cl}_{11}]$, and a mixture of $[(\text{Me}_3\text{Si})_2\text{NTf}_2][\text{HCB}_{11}\text{Cl}_{11}]$ (1 eq) with Me_3SiOTf (0.95 eq). Note that the peak around -113 ppm in the $[(\text{Me}_3\text{Si})_2\text{OTf}][\text{HCB}_{11}\text{Cl}_{11}]$ spectrum is PhF.

Equilibrium of $[(\text{Me}_3\text{Si})_2\text{NTf}_2][\text{HCB}_{11}\text{Cl}_{11}]$ with Me_3SiOTf in $\text{C}_7\text{D}_8/\text{ODCB}$ at various temperatures. A stock solution was created of SiMe_4 (125 μL), ODCB (9 mL), and C_7D_8 (1 mL) using micro syringes. In a J. Young, a ~ 120 mM solution of a substrate (Me_3SiOTf , $\text{Me}_3\text{SiNTf}_2$, $[(\text{Me}_3\text{Si})_2\text{OTf}][\text{HCB}_{11}\text{Cl}_{11}]$, or $[(\text{Me}_3\text{Si})_2\text{NTf}_2][\text{HCB}_{11}\text{Cl}_{11}]$) was made using the stock solution as a solvent. The $^{29}\text{Si}\{^1\text{H}\}$ NMR chemical shift was examined for each substrate using variable temperature NMR (VT NMR) with the TMS peak always being referenced to 0 ppm. To another J. Young tube, $[(\text{Me}_3\text{Si})_2\text{NTf}_2][\text{HCB}_{11}\text{Cl}_{11}]$ (70 mg, 0.074 mmol) and Me_3SiOTf (~ 13.25 μL , 0.073 mmol) were combined with 600 μL of the stock solution. The mixture was analyzed by ^{19}F NMR revealing the actual molar ratio of Me_3SiOTf that was added relative to $[(\text{Me}_3\text{Si})_2\text{NTf}_2][\text{HCB}_{11}\text{Cl}_{11}]$ was 0.65 to 1.0 respectively. The $^{29}\text{Si}\{^1\text{H}\}$ chemical shift was examined by VT at 20, 40, 60, 80, and 100 $^\circ\text{C}$. The K_{eq} was calculated using the same equations listed before and a Van't Hoff analysis suggested a ΔH of 1.1 ± 0.4 kcal/mol and a ΔS of 4.5 ± 1.1 cal/(mol \times K).



Table S2. $^{29}Si\{^1H\}$ NMR chemical shifts and calculated K_{eq} at various temperatures.

Temp (Kelvin)	$\delta^{29}Si\{^1H\}$ Chemical Shift of $[(Me_3Si)_2NTf_2][Cl_{11}]$ (ppm)	$\delta^{29}Si\{^1H\}$ Chemical Shift of Me_3SiOTf	$\delta^{29}Si\{^1H\}$ Chemical Shift of $[(Me_3Si)_2OTf][Cl_{11}]$	$\delta^{29}Si\{^1H\}$ Chemical Shift of Me_3SiNTf_2	$\delta^{29}Si\{^1H\}$ Chemical Shift of Equilibrium	K_{eq} ($[C][D]/[A][B]$)
293.1	73.03	43.69	75.95	55.66	65.45	1.5±0.4
313.1	73.17	43.49*	76.18	55.46	65.55	1.6±0.5
333.2	73.36	43.29	76.40	55.27	65.67	1.8±0.5
353.1	73.54	43.12*	76.62	55.07	65.81	2.0±0.6
373.2	73.71	42.93	76.85	54.89	65.94	2.3±0.7

*Predicted $^{29}Si\{^1H\}$ values based on linear interpolation

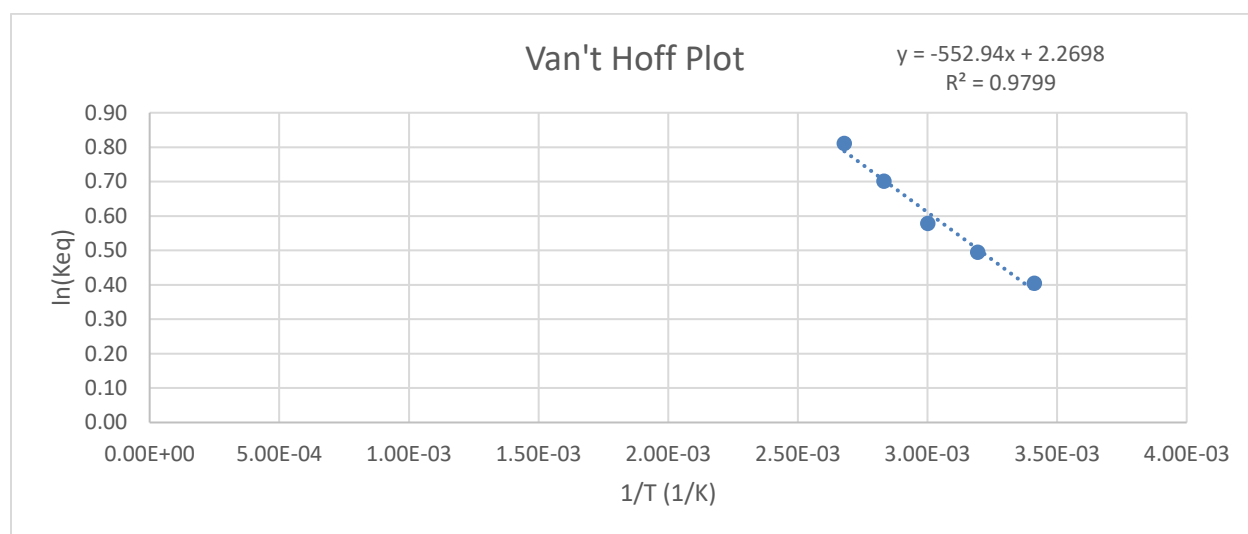


Figure S12. Van't Hoff analysis of equilibrium.

V. Characterization Details

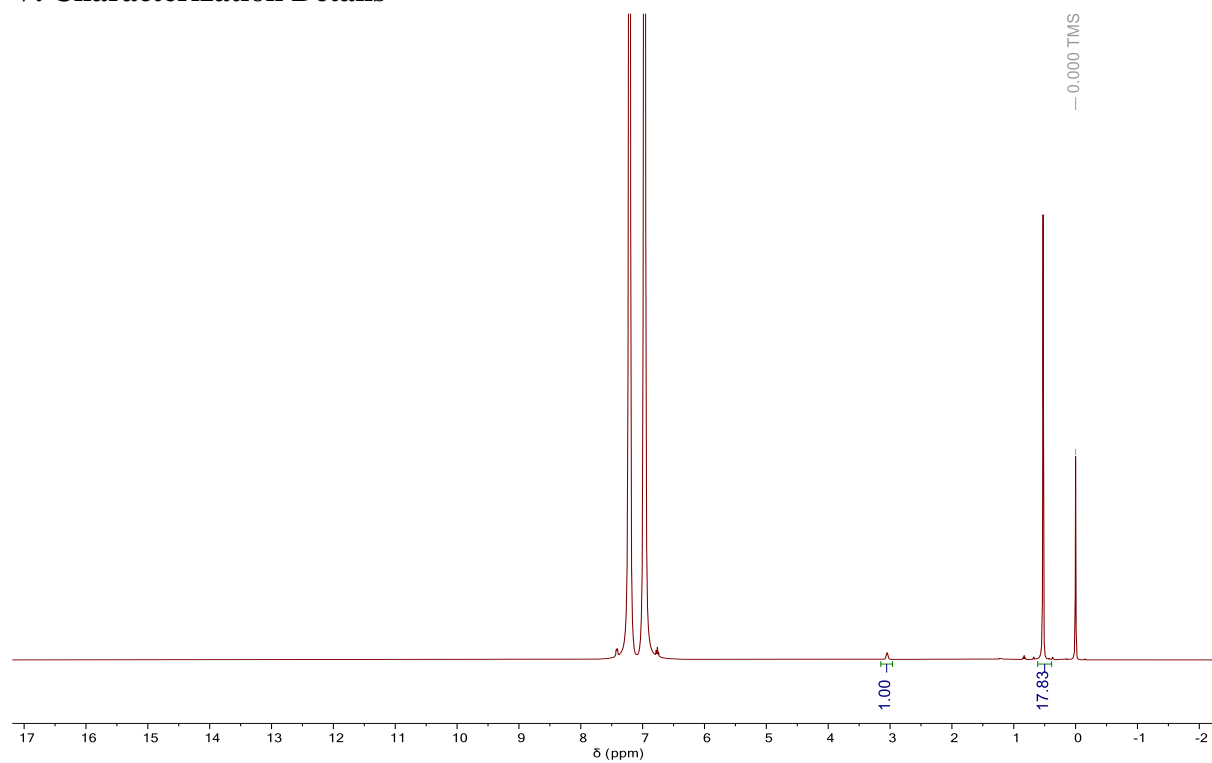


Figure S13. ^1H NMR (400 MHz/ODCB/unlocked) spectrum of $[(\text{Me}_3\text{Si})_2\text{NTf}_2][\text{HCB}_{11}\text{Cl}_{11}]$. Note that SiMe_4 has been added as a reference.

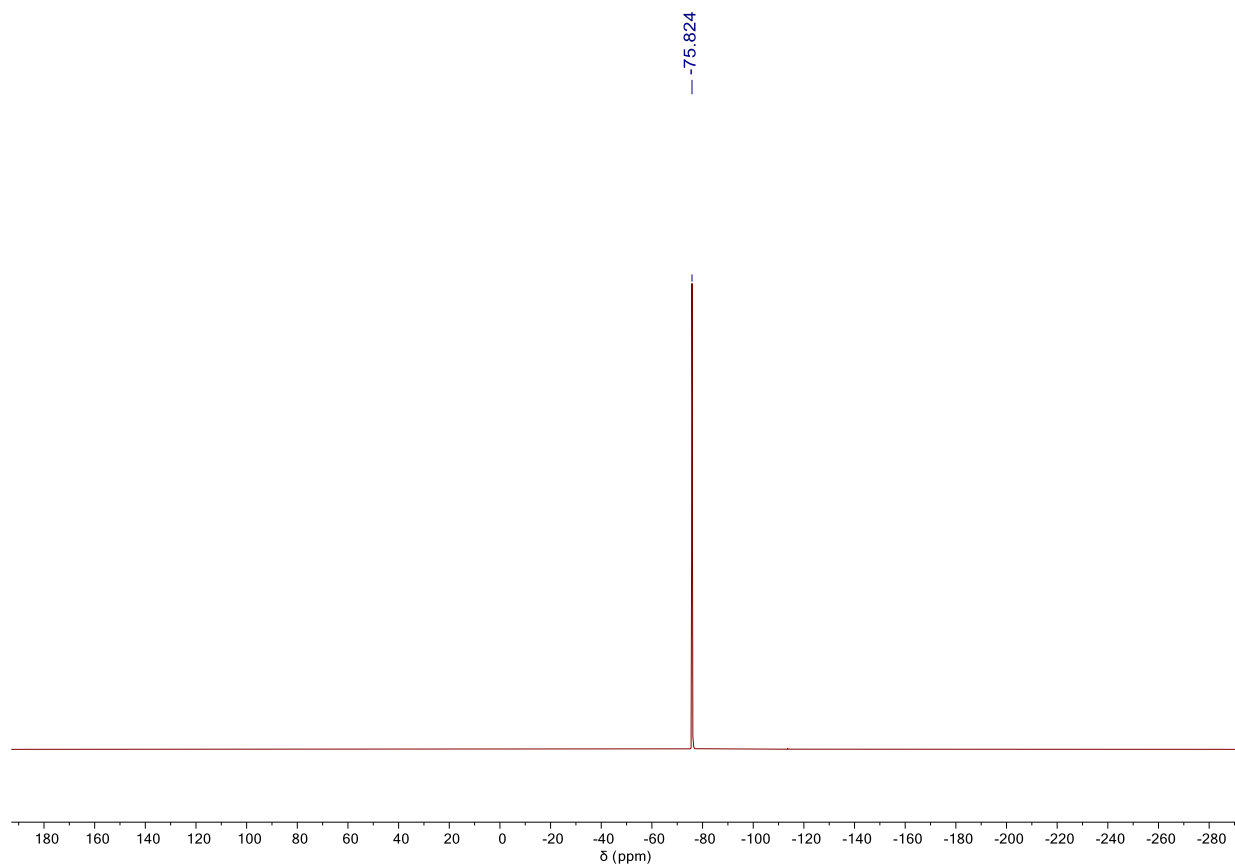


Figure S14. ^{19}F NMR (162 MHz/ODCB/unlocked) spectrum of $[(\text{Me}_3\text{Si})_2\text{NTf}_2][\text{HCB}_{11}\text{Cl}_{11}]$.

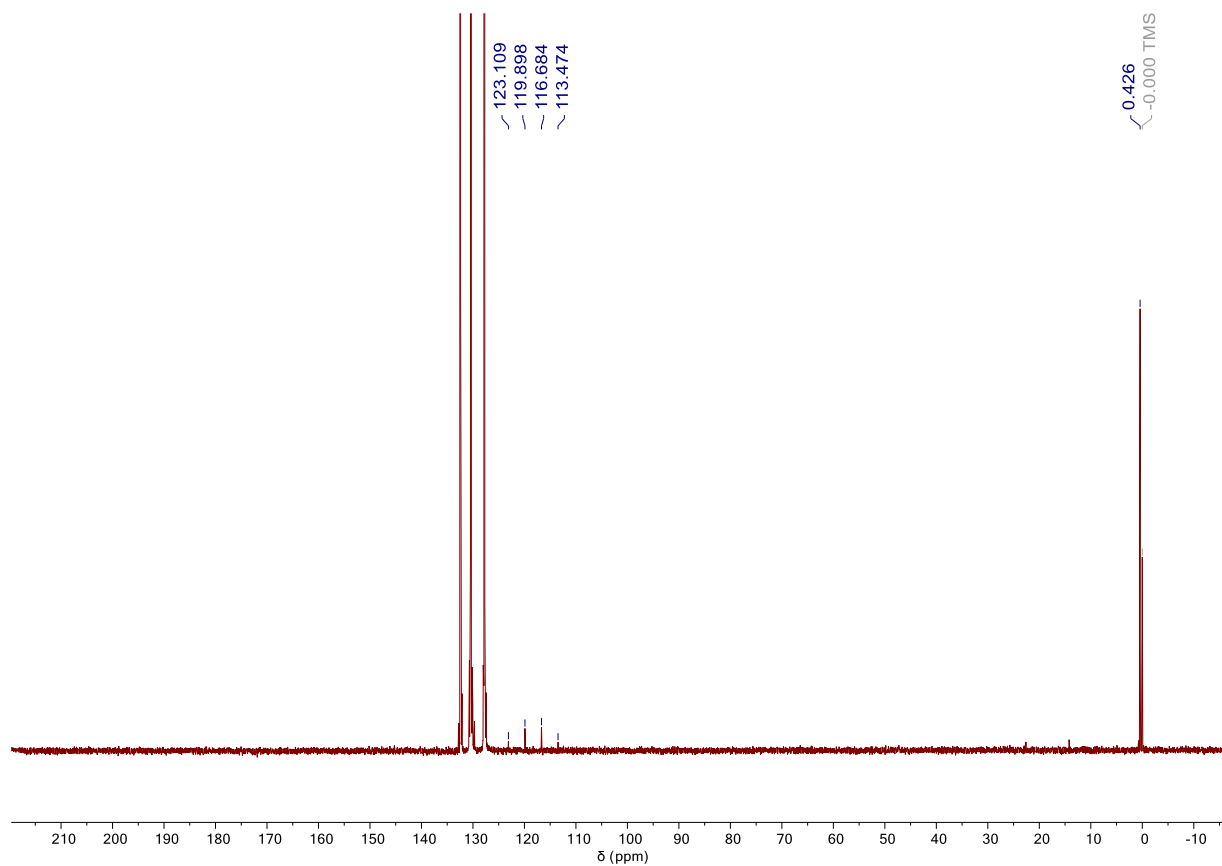


Figure S15. $^{13}\text{C}\{^1\text{H}\}$ NMR (101 MHz/ODCB/unlocked) spectrum of $[(\text{Me}_3\text{Si})_2\text{NTf}_2][\text{HCB}_{11}\text{Cl}_{11}]$. Note that SiMe_4 has been added as a reference.

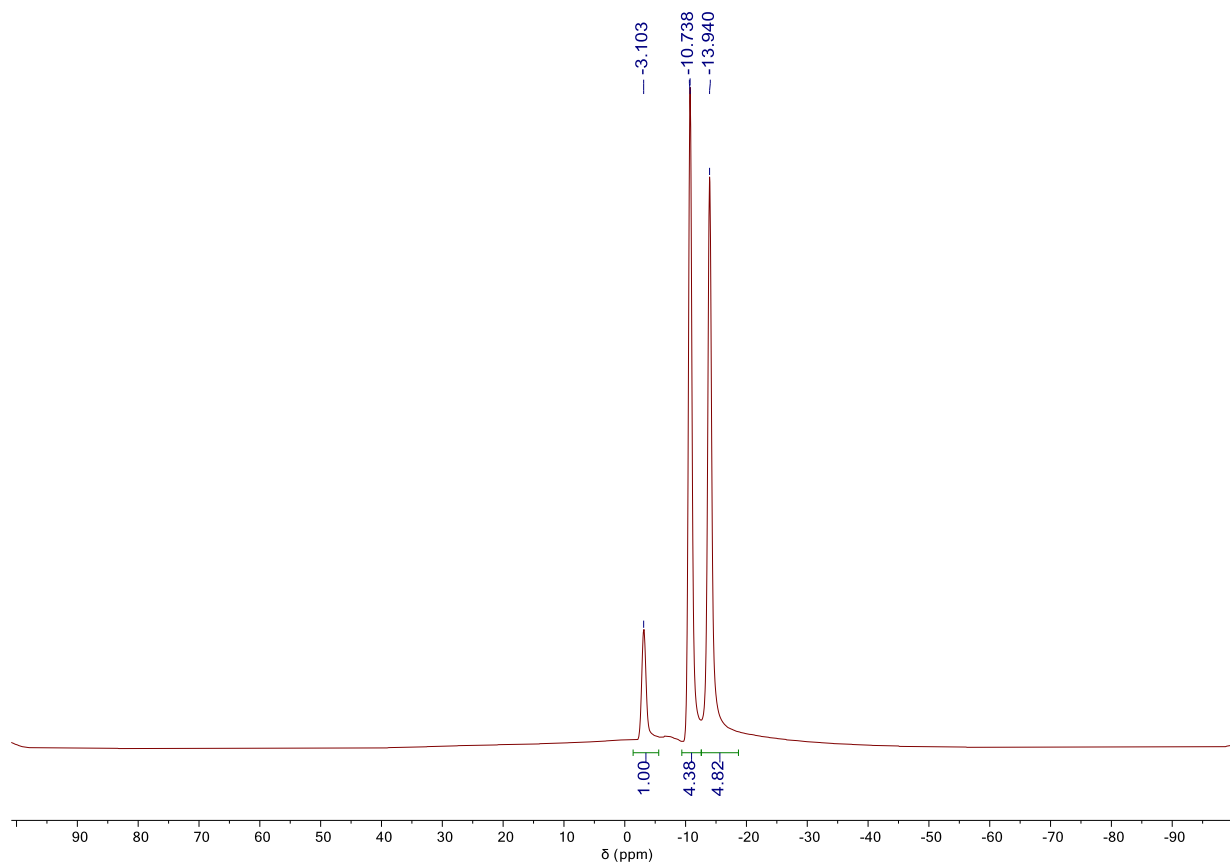


Figure S16. $^{11}\text{B}\{^1\text{H}\}$ NMR (128 MHz/ODCB/unlocked) spectrum of $[(\text{Me}_3\text{Si})_2\text{NTf}_2][\text{HCB}_{11}\text{Cl}_{11}]$.

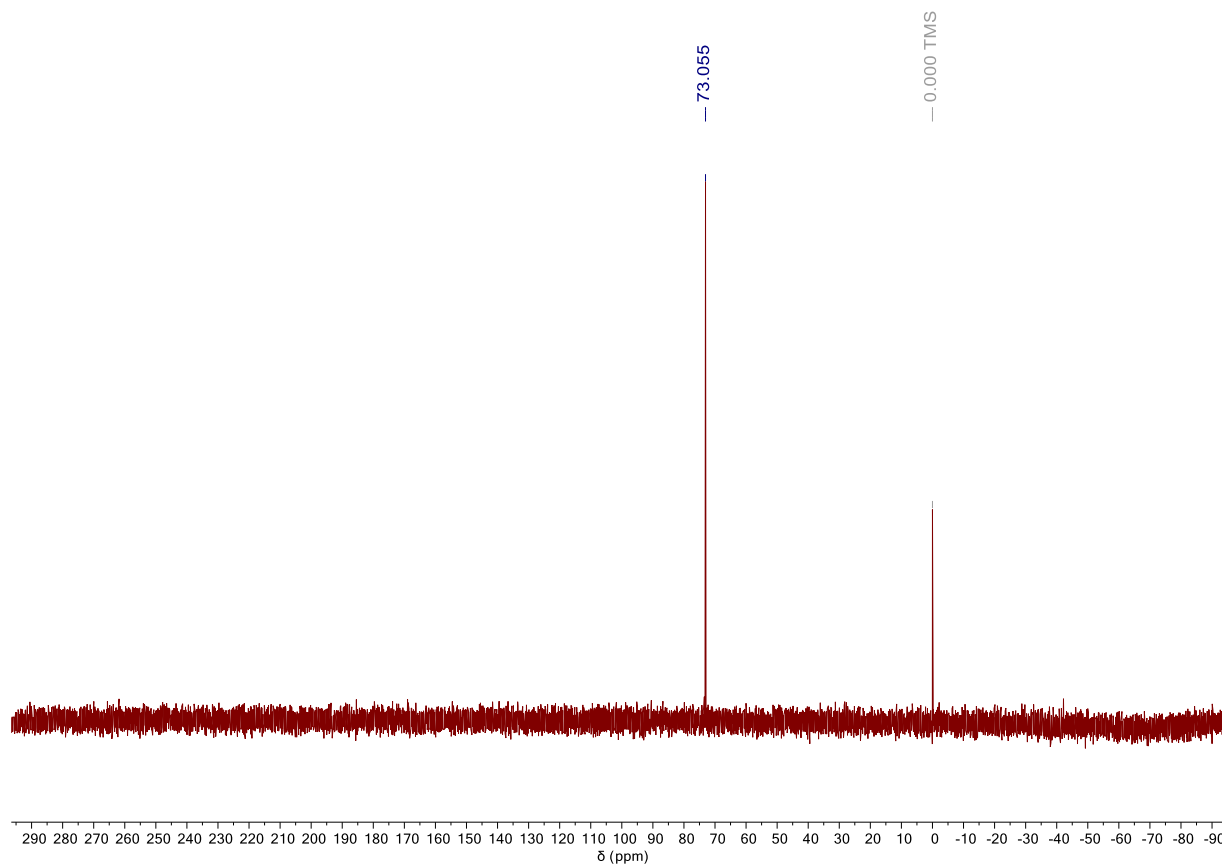


Figure S17. $^{29}\text{Si}\{^1\text{H}\}$ NMR (79 MHz/ODCB/unlocked) spectrum of $[(\text{Me}_3\text{Si})_2\text{NTf}_2][\text{HCB}_{11}\text{Cl}_{11}]$. Note that SiMe_4 has been added as a reference.

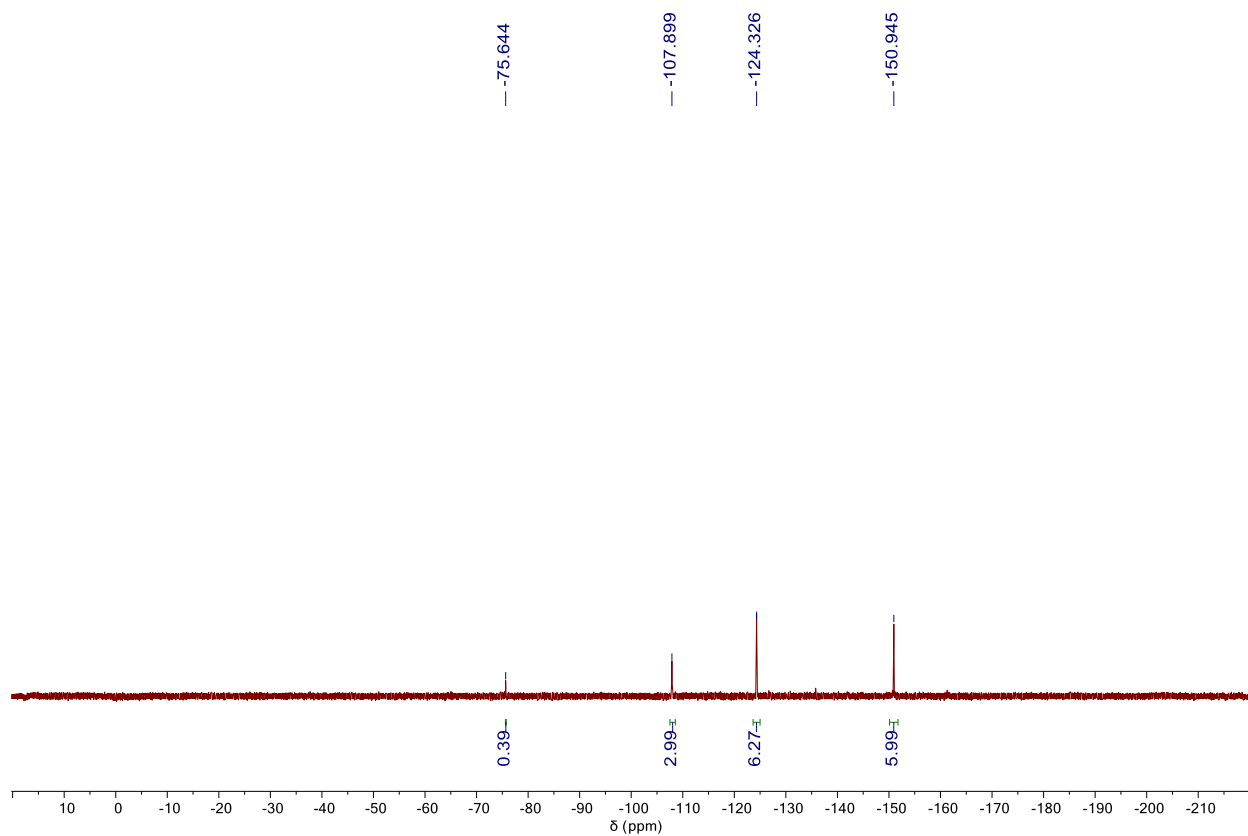


Figure S18. ^{19}F NMR (376 MHz/ SO_2Cl_2 /unlocked) spectrum of $[\text{F}_{15}\text{Tr}][\text{HCB}_{11}\text{Cl}_{11}]$ made from reacting $[(\text{Me}_3\text{Si})_2\text{NTf}_2][\text{HCB}_{11}\text{Cl}_{11}]$ with $\text{F}_{15}\text{Tr}\text{-OTFA}$. The peak at -75.6 ppm is trace amount of unreacted $[(\text{Me}_3\text{Si})_2\text{NTf}_2][\text{HCB}_{11}\text{Cl}_{11}]$.

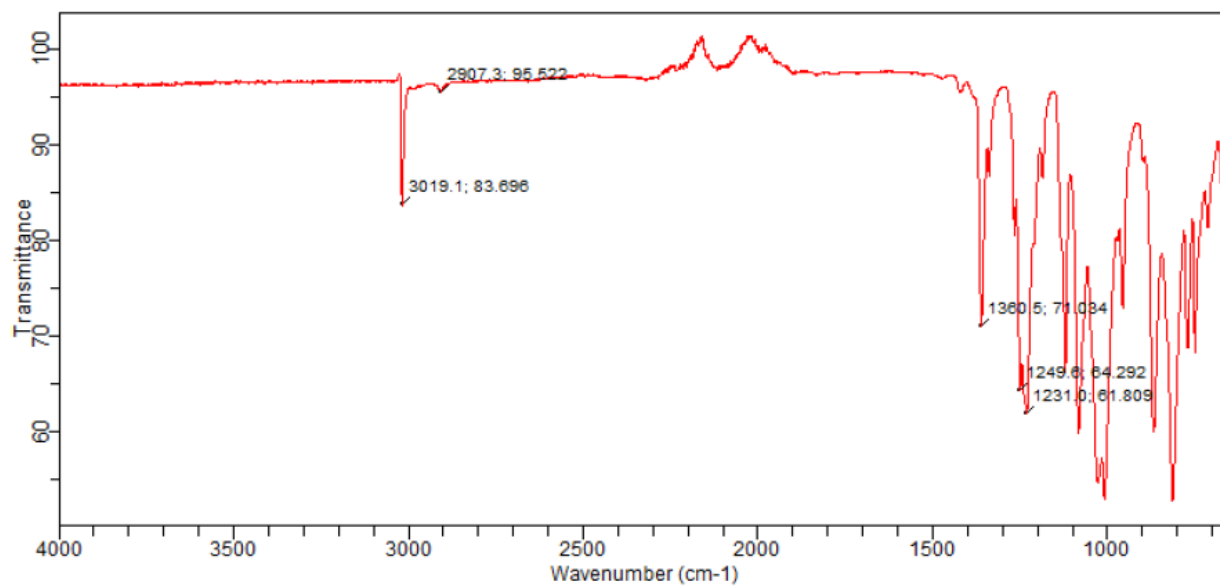


Figure S19. FTIR of $[(\text{Me}_3\text{Si})_2\text{NTf}_2][\text{HCB}_{11}\text{Cl}_{11}]$ final product.

VI. X-Ray Structural Analysis

X-Ray data collection, reduction, solution, and refinement of $[(\text{Me}_3\text{Si})_2\text{NTf}_2][\text{HCB}_{11}\text{Cl}_{11}]$ (CCDC 2428563)

A Leica M80 microscope was used to identify a suitable single colorless block-shaped crystal of $[(\text{Me}_3\text{Si})_2\text{NTf}_2][\text{HCB}_{11}\text{Cl}_{11}]$ showing well defined faces with dimensions $0.33 \times 0.09 \times 0.08 \text{ mm}^3$ from a representative sample of crystals of the same habit. The crystal mounted on a nylon loop was then placed in a cold nitrogen stream (Oxford) maintained at $T = 100.0(3) \text{ K}$.

Crystal screening, unit cell determination, and data collection were carried out using a XtaLAB Synergy, Dualflex, HyPix diffractometer. The diffraction pattern was indexed and the total number of runs and images was based on the strategy calculation from the program CrysAlisPro system.⁵ Data were measured using ω scans with Cu K_α radiation. Data was collected to a maximum resolution of $Q = 70.070^\circ$ (0.82 \AA). The unit cell was refined using CrysAlisPro 1.171.43.98a¹ on 39593 reflections, 57 % of the observed reflections.

Integrated Intensity information for each reflection was obtained by reduction of data frames using CrysAlisPro 1.171.43.98a.⁵ The final completeness is 99.80 % out to 70.070° in Q . A gaussian absorption correction was performed using CrysAlisPro 1.171.43.98a.⁵ Numerical absorption correction based on gaussian integration over a multifaceted crystal model Empirical absorption correction using spherical harmonics, implemented in SCALE3 ABSPACK scaling algorithm. The absorption coefficient m of this material is 9.635 mm^{-1} at this wavelength ($\lambda = 1.54184 \text{ \AA}$) and the minimum and maximum transmissions are 0.387 and 1.000.

Systematic reflection conditions and statistical tests of the data suggested the space group $P-1$ (# 2) and was confirmed by ShelXT 2018/2⁶ structure solution program using dual methods. The

structure was refined by full matrix least squares minimization on F^2 using version 2019/1 of ShelXL 2019/1.⁷ All non-hydrogen atoms were refined anisotropically. Hydrogen atom positions were calculated geometrically and refined using the riding model.

VII. References

-
- ¹ S. O. Gunther, C.-I. Lee, E. Song, N. Bhuvanesh and O. V. Ozerov, *Chem. Sci.*, 2022, **13**, 4972–4976.
- ² D. W. Leong, A. R. Gogoi, T. Maity, C.-I. Lee, N. Bhuvanesh, O. Gutierrez and O. V. Ozerov, *Angew. Chem. Int. Ed.*, 2025, e202422190.
- ³ N. Gnyra, 2017, *Propagation of uncertainty calculator*, <https://github.com/nicoco007/Propagation-of-Uncertainty-Calculator>.
- ⁴ D. N. Gardner, H. Williams, S. C. Vogel, S. Fayfar, B. Khaykovich, S. Srivastava, A. Hwang, M. Asta, D. Sprouster, D. Olds, G. Vershbow, J. C. Neufeind and R. O. Scarlat, *J Appl Cryst*, 2025, **58**, 435–446.
- ⁵ Rigaku Oxford Diffraction, CrysAlisPro Software System.
- ⁶ G. M. Sheldrick and SHELXT, *Acta Cryst A*, 2015, **71**, 3–8.
- ⁷ G. M. Sheldrick, *Acta Crystallogr. Sect. C Struct. Chem.*, 2015, **71**, 3–8.